Closed-Loop Control of Functional Neuromuscular Stimulation

NIH Neuroprosthesis Program Contract Number N01-NS-6-2338
Quarterly Progress Report #14
July 1, 1999 to September 30, 1999

Investigators:
Patrick E. Crago, Ph.D.
Clayton L. Van Doren, Ph.D.
Warren M. Grill, Ph.D.
Michael W. Keith, M.D.
Kevin L. Kilgore, Ph.D.
Joseph M. Mansour, Ph.D.
Wendy M. Murray, PhD.
P. Hunter Peckham, Ph.D.
David L. Wilson, Ph.D.

Cleveland FES Center

Departments of Biomedical Engineering,
Mechanical and Aerospace Engineering,
and Orthopaedics
Case Western Reserve University
and MetroHealth Medical Center

1. SYNTHESIS OF UPPER EXTREMITY FUNCTION 3

1. A. BIOMECHANICAL MODELING: PARAMETERIZATION AND VALIDATION 3
Purpose 3
Progress Report 3
1. a. i. MOMENT ARMS VIA MAGNETIC RESONANCE IMAGING 3
Abstract 3
1.a.ii. PASSIVE AND ACTIVE MOMENTS 3
Abstract 3
Purpose 3
Progress Report 3
Plans for Next Quarter 4
1. B. BIOMECHANICAL MODELING: ANALYSIS AND IMPROVEMENT OF GRASP OUTPUT 4
Abstract 4
Purpose 4
Progress Report 4
Report of Progress 7
Plans for Next Quarter 13

2. CONTROL OF UPPER EXTREMITY FUNCTION 13

2. A. HOME EVALUATION OF CLOSED-LOOP CONTROL AND SENSORY FEEDBACK 14
Abstract 14
Purpose 14
Progress Report 14
Plans for Next Quarter 14
2. b. i. ASSESSMENT OF SENSORY FEEDBACK IN THE PRESENCE OF VISION 14
Abstract 14
Purpose 14
Plans for Next Quarter 19
2. b. ii. INNOVATIVE METHODS OF COMMAND CONTROL 19
Abstract 19
Purpose 19
Progress Report 20
Plans for Next Quarter 24
2. b. iii. INCREASING WORKSPACE AND REPERTOIRE WITH BIMANUAL HAND GRASP 24
Abstract 24
Purpose 24
Progress Report 24
Plans for Next Quarter 27
2. b. iv CONTROL OF HAND AND WRIST 27
Abstract 27
Purpose 28
Progress Report 28
Plans for next quarter 30

1. SYNTHESIS OF UPPER EXTREMITY FUNCTION

The overall goals of this project are to (1) measure the biomechanical properties of the neuroprosthesis user's upper extremity and incorporate those measurements into a complete model with robust predictive capability, and (2) use the predictions of the model to improve the grasp output of the hand neuroprosthesis for individual users.

1. a. BIOMECHANICAL MODELING: PARAMETERIZATION AND VALIDATION

Purpose

In this section of the contract, we will develop methods for obtaining biomechanical data from individual persons. Individualized data will form the basis for model-assisted implementation of upper extremity FNS. Using individualized biomechanical models, specific treatment procedures will be evaluated for individuals. The person-specific parameters of interest are tendon moment arms and lines of action, passive moments, and maximum active joint moments. Passive moments will be decomposed into components arising from stiffness inherent to a joint and from passive stretching of muscle-tendon units that cross one or more joints.

Progress Report

1. a. i. MOMENT ARMS VIA MAGNETIC RESONANCE IMAGING

Abstract

No activity took place with regard to this project this quarter.

1.a.ii. PASSIVE AND ACTIVE MOMENTS

Abstract

During this quarter, a manuscript on the technique for separating passive moments was submitted to the Journal of Biomechanics.

Purpose

The purpose of this project is to characterize the passive properties of normal and paralyzed hands. This information will be used to determine methods of improving hand grasp and hand posture in FES systems.

Progress Report

During this quarter, a manuscript was submitted to Journal of Biomechanics.

Jayme S. Knutson, Kevin L. Kilgore, Joseph M. Mansour, and Patrick E. Crago, Separating Passive Joint Moment into Intrinsic and Extrinsic Components.

ABSTRACT

The passive moment about the metacarpophalangeal (MP) joint of the index finger was modeled as the sum of components that are produced by tissues intrinsic and extrinsic to the joint. This allows quantification of the contribution of these two tissue groups to the total passive resistance to joint

rotation. A series of passive moment measurements were made at the MP joint of the index finger in 8 subjects. The passive moment was recorded while the finger was rotated at a constant rate of 50 deg s^{-1} and with the wrist fixed in seven different flexion-extension angles. The moment-angle data from each individual was fit to an equation that models the passive moment as the sum of wrist-angle-independent (intrinsic) and wrist-angle-dependent (extrinsic) components. The former is produced by ligaments and tissues that compose the MP joint capsule, and the latter is produced by extrinsic muscle-tendon units that span both the wrist and the MP joint. For 8 subjects the percent contributions of these two tissue groups to the overall joint resistance were calculated. The median percent extrinsic contribution to a 40 N-cm MP joint extension moment was 94% with the wrist extended 60° and 14% with the wrist flexed 60°. These percentages were 40% and 88%, respectively, for a –40 N-cm joint moment (flexion). This model can assist in diagnosing the source of contractures or other adverse joint properties and for monitoring the effects of therapy. A clinical example demonstrating the utility of the model is presented.

Plans for Next Quarter

During the next quarter, we will perform experiments to examine the effect of the position of the proximal interphalangeal joint on the MP joint properties.

1. b. BIOMECHANICAL MODELING: ANALYSIS AND IMPROVEMENT OF GRASP OUTPUT

Abstract

The Br-ECRB tendon transfer is intended to restore voluntary wrist extension after cervical spinal cord injury. There is a limited amount of quantitative information in the literature that characterizes wrist function after a Br-ECRB tendon transfer. Previous progress reports have described limitations in wrist function after the Br-ECRB that are predicted using a biomechanical model of the elbow and wrist. In order to verify the biomechanical model predictions, to evaluate how post-operative wrist function could be improved, and to identify issues for further study, we have collected and evaluated clinical assessments of wrist function in 16 wrists with Br-ECRB transfers.

Purpose

The purpose of this project is to use the biomechanical model and the parameters measured for individual neuroprosthesis users to analyze and refine their neuroprosthetic grasp patterns.

In the past quarter, we have evaluated how the passive moment-generating capacity of the tight and slack Br-ECRB transfer (described in previous progress reports) influences gravity-assisted wrist flexion. The net passive moment at the wrist joint (before a Br-ECRB transfer) was compared to the passive wrist extension moment generated by the transfer to estimate the range of wrist postures where gravity-assisted wrist flexion is possible.

Progress Report

In the past quarter, we have continued to evaluate patient data from our clinical research laboratory to assess wrist function after the Br-ECRB tendon transfer. In particular, we have focused on quantifying the differences in wrist function across subjects and investigating potential sources of these differences. In addition, Wendy Murray traveled to the 1999 American Society of Biomechanics Conference in Pittsburgh, PA and gave a podium presentation entitled “Wrist Function after the Br-ECRB Tendon Transfer.” The abstract follows.

WRIST FUNCTION AFTER THE BR-ECRB TENDON TRANSFER

Wendy M. Murray, Kevin L. Kilgore, Michael W. Keith
Biomedical Engineering Department and Cleveland FES Center
Case Western Reserve University and MetroHealth Medical Center
Cleveland, OH
Email: wmm@po.cwru.edu

INTRODUCTION

The ability to extend and flex the wrist is essential for providing functional use of the hand to persons with tetraplegia (quadriplegia). Wrist extension closes the hand and wrist flexion opens the hand, providing a means to grasp and release light objects. Individuals with a spinal cord injury at the fifth cervical segment (C5) have severely weakened or paralyzed wrist extensors, as well as paralyzed wrist flexors (Long and Lawton, 1955). Surgically attaching the distal tendon of the brachioradialis (Br), an intact elbow flexor, to the distal tendon of the extensor carpi radialis brevis (ECRB), a paralyzed wrist extensor, provides a means to voluntarily extend the wrist. Once active wrist extension is restored, gravity can assist passive wrist flexion.

The ability to extend the wrist does not always improve after the Br-ECRB tendon transfer (Freehafer and Mast, 1967). Also, a reduction in the passive range of motion at the wrist has been observed after transfer (Johnson et al., 1996). We hypothesize that surgical tensioning of the Br-ECRB transfer influences both active wrist extension and passive range of motion. We have developed a computer simulation of the transfer to test this hypothesis and to evaluate how surgical technique influences wrist function.

PROCEDURES

The Br-ECRB tendon transfer was simulated using an existing computer graphics-based model of the upper extremity (Murray *et al.*, 1995; Gonzalez *et al.*, 1997). The computer model allows the calculation of muscle lengths, forces, moment arms, and joint moments as a function of both elbow and wrist position. The model of the Br-ECRB transfer assumes that the transfer combines the elbow flexion moment arm of the brachioradialis with the wrist extension moment arm of the ECRB. We used the model to evaluate two different surgical techniques. The model of a *slack* transfer assumes the muscle fibers operate primarily on the ascending limb and plateau of the isometric force-length curve between full elbow extension (0˚) and 130˚ elbow flexion. The model of a *tight* transfer assumes the muscle fibers operate at longer lengths for this range of motion, on the plateau and descending limb of the force-length curve.

To evaluate how surgical technique influences wrist function, the active and passive moment-generating capacities of the slack and tight transfers were compared to passive properties of the wrist joint. Wrist function was evaluated in arm postures where gravity opposes wrist extension. The gravitational wrist flexion moment imposed by the weight of the hand was estimated for a 50th percentile male based on regression equations (McConville et al., 1980), and was combined with measurements of the passive moment generated at the wrist by joint structures and muscles. Passive joint properties were measured in a subject with C5 level tetraplegia (Lemay and Crago, 1997).

RESULTS AND DISCUSSION

Given the passive wrist joint properties of an individual with C5 level tetraplegia without a Br-ECRB tendon transfer, the equilibrium position of the wrist (i.e., the position where the net passive moment is 0 Nm) is 26˚ flexion (Fig. 1). In more flexed wrist positions, the net passive moment is an extension moment. Thus, without the ability to actively generate a flexion moment, 26˚ flexion is the most flexed wrist posture that can be reached.

When the elbow is fully extended, both the slack and tight transfers generate a passive wrist extension moment which limits the attainable range of motion (Fig. 1). The passive extension moment generated by

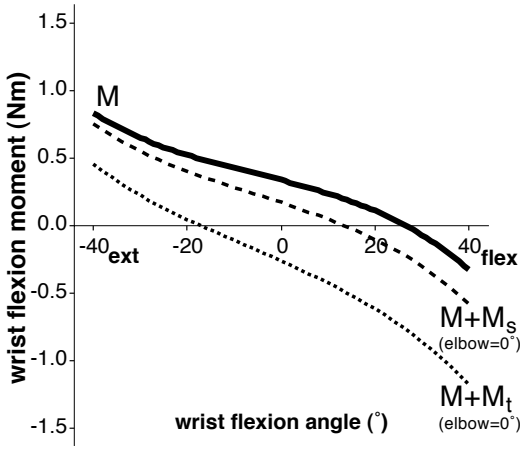

Figure 1. Net passive moment at the wrist joint without the Br-ECRB transfer (M), after a slack transfer ($M+M_s$), and after a tight transfer ($M+M_t$).

the slack transfer shifts the equilibrium position (and maximum flexion position) of the wrist to 12˚ flexion. The tight transfer shifts the equilibrium position to 18˚ wrist *extension*.

To maintain the wrist in a posture that is more extended than its equilibrium position, the Br-ECRB transfer must generate an extension moment to balance the net passive flexion moment at the wrist. The maximum isometric wrist extension moment generated by the transfer varies as a function of both wrist and elbow position. When the wrist is extended 40˚, the moment-generating capacity of the slack transfer is not sufficient to maintain this wrist posture at elbow flexion angles greater than 108˚ (Fig. 2). However, the tight transfer can maintain 40˚ wrist extension up to 128˚ elbow flexion.

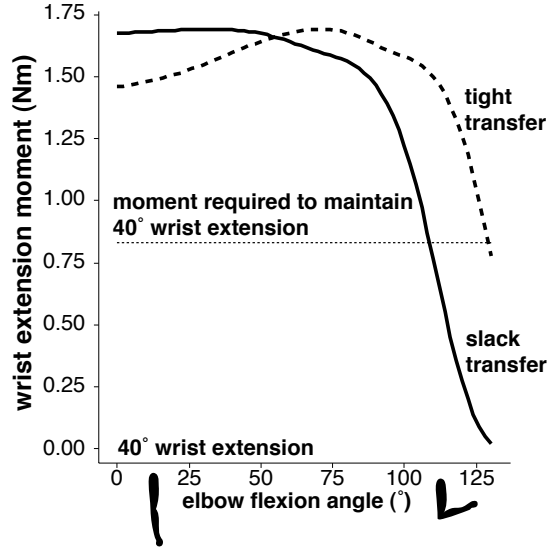

Figure 2. Comparison between the wrist extension moment generated by the slack and tight transfers when the wrist is extended 40˚ with the joint moment required to maintain that position.

SUMMARY

Surgical tensioning of the Br-ECRB transfer influences the ability to actively extend the wrist and the passive range of motion of the wrist. When tensioning the Br-ECRB tendon transfer, a surgeon should consider the balance between wrist extension (which provides *hand grasp*) and wrist flexion (which provides *hand opening*) that is necessary for functional use of the hand.

REFERENCES

Freehafer, A. A. and Mast, W. A. (1967). *J Bone Jt Surg*, **49-A,** 648-652.
Gonzalez, R. V. et al. (1997). *J Biomech*, **30,** 705-712.
Johnson, D. L. et al. (1996). *J Bone Jt Surg*, **78-A,** 1063-1067.
Lemay, M. A., and Crago, P. E. (1997). *IEEE Trans Rehab Eng*, **5,** 244-252.
Long, C. and Lawton, E. B. (1955). *Arch Phys Med Rehab*, **36,** 249-255.
McConville, J. T. et al. (1980). *Technical Report AFAMRL-TR-80-119*.
Murray, W. M. et al. (1995). *J Biomech*, **28,** 513-525.

Report of Progress

In the past quarter, we have continued to evaluate patient data from our clinical research laboratory to assess wrist function after the Br-ECRB tendon transfer. In particular, we have focused on quantifying the differences in wrist function across subjects and investigating potential sources of these differences. In addition, Wendy Murray traveled to the 1999 American Society of Biomechanics Conference in Pittsburgh, PA and gave a podium presentation entitled "Wrist Function after the Br-ECRB Tendon Transfer." The two page abstract is included with this progress report.

Evaluating the Br-ECRB tendon transfer in patients

A follow-up of Br-ECRB tendon transfer patients is being carried out in our clinical laboratory. The objectives of the clinical evaluations are to characterize wrist function after the Br-ECRB tendon transfer, to identify aspects of wrist function after the transfer that need improvement, and to evaluate potential causes of the different outcomes.

The maximum wrist extension position that could be voluntarily maintained against gravity varied considerably in 16 wrists (from 14 individuals) with Br-ECRB transfers. The maximum position that could be actively maintained against gravity ranged from 75˚ extension to 40˚ flexion; three individuals could not actively position their wrists in an extended posture against gravity post-operatively (Fig. 1.b.1A). Likewise, the passive limit of wrist extension differed across wrists. However, all 16 wrists could passively be positioned in wrist extension. The passive limit ranged from 90˚ wrist extension to 6˚ wrist extension (Fig. 1.b.1B).

To compare function across the 16 wrists, we normalized the active range of motion in wrist extension by the passive range of wrist extension. We categorized the wrists into three groups based on this normalization. In Group I, active wrist extension against gravity approached the limits of the available passive range of motion. In Group II, there was room for improvement in active extension relative to the passive range of motion. In Group III, there were substantial deficits in active wrist extension. Specifically, in seven wrists (Group I), the active range of motion (AROM) was greater than 75% of the available passive range of motion (PROM, Fig. 1.b.2). On average, the maximum position in extension that could be maintained against gravity was within 9˚ of the passive limit of wrist extension in these wrists. In five wrists (Group II), the AROM was greater than 50% but less than 75% of the available passive range of motion. On average, the maximum position that could be maintained against gravity was within 22˚ of the passive limit of extension in these wrists. In four wrists (Group III), the AROM was less than 50% of the available passive range of motion. On average, the maximum position that could be maintained against gravity was less than the passive limit of wrist extension by 54˚.

In some wrists, the passive range of motion could be the factor limiting active wrist extension. Active wrist extension against gravity approached the limits of the available passive range of motion for the seven wrists in Group I. However, the passive limit of wrist extension in Group I ranged from 32˚ wrist extension to 90˚ wrist extension. In the 12 wrists in Groups I and II, there was a significant correlation between the active range of motion in extension and the passive range of motion ($r = 0.881$; $p < 0.0002$). The variability in the passive range of motion accounted for 78% of the variation in active range of motion in these 12 wrists (Fig. 1.b.3).

Another factor that could limit active wrist extension post-operatively is muscle strength. Clinically, muscle strength is evaluated using manual muscle tests, which rely on observations of muscle contraction and the resultant movement of the joint. A manual muscle test score of 5 indicates a clinical assessment of normal strength. If the muscle is observed to be weaker than this subjective assessment of normal, but can still move the joint through its range of motion against gravity and resistance, the muscle is graded as a 4. A score of 3 indicates active movement occurs against gravity. If active movement only occurs when gravity is eliminated, the manual muscle test score is 2. A trace of a contraction is graded as a 1, and a 0 indicates no contraction was observed. In the 16 wrists with Br-ECRB tendon transfers summarized here, pre-operative manual muscle tests were performed at the elbow and wrist to evaluate the strength of the brachioradialis and the residual strength of the wrist extensors, respectively. Post-operative manual muscle tests were performed at the wrist to assess post-operative wrist extension strength. The pre-operative manual muscle tests did not predict the functional outcome of the transfer. Specifically, there were no significant differences in the manual muscle test scores assigned to brachioradialis pre-operatively (Fig. 1.b.4A) or to the pre-operative residual strength of the wrist extensors across Group I, Group II, and Group III (Fig. 1.b.4B). Similarly, the post-operative manual muscle tests did not discriminate between the functional outcomes. There were no significant differences in the post-operative manual muscle test scores for wrist extension across Group I, Group II, and Group III (Fig. 1.b.5).

Summary

Clinical evaluations of wrist function after the Br-ECRB transfer indicate that both the active and passive ranges of motion vary considerably across wrists post-operatively. By normalizing the active range of motion in wrist extension by the available passive range of motion, we distinguished between three subsets of post-operative wrist function; a group where active wrist extension approached the limits of the passive range of motion (Group I), a group where active wrist extension was severely limited relative to the available passive range of wrist extension (Group III), and a group intermediate to these two groups (Group II). Even across the two groups that had higher levels of post-operative function (Group I and Group II), there was a broad range of active and passive ranges of motion. Active range of motion was significantly correlated to passive range of motion in the 12 wrists in Groups I and II, indicating that passive range of motion could be an important factor limiting post-operative wrist extension in some wrists. There were no significant differences in pre-operative brachioradialis strength, pre-operative wrist extension strength, and post-operative wrist extension strength across the three groups, as measured clinically using the manual muscle test. The result that post-operative differences in wrist function are not related to differences in muscle strength is counterintuitive. Because the manual muscle test is a subjective measure of muscle strength, this result warrants further investigation. In the future, we will evaluate differences in strength across subjects using more objective tools, such as the elbow and wrist moment transducers described in previous progress reports.

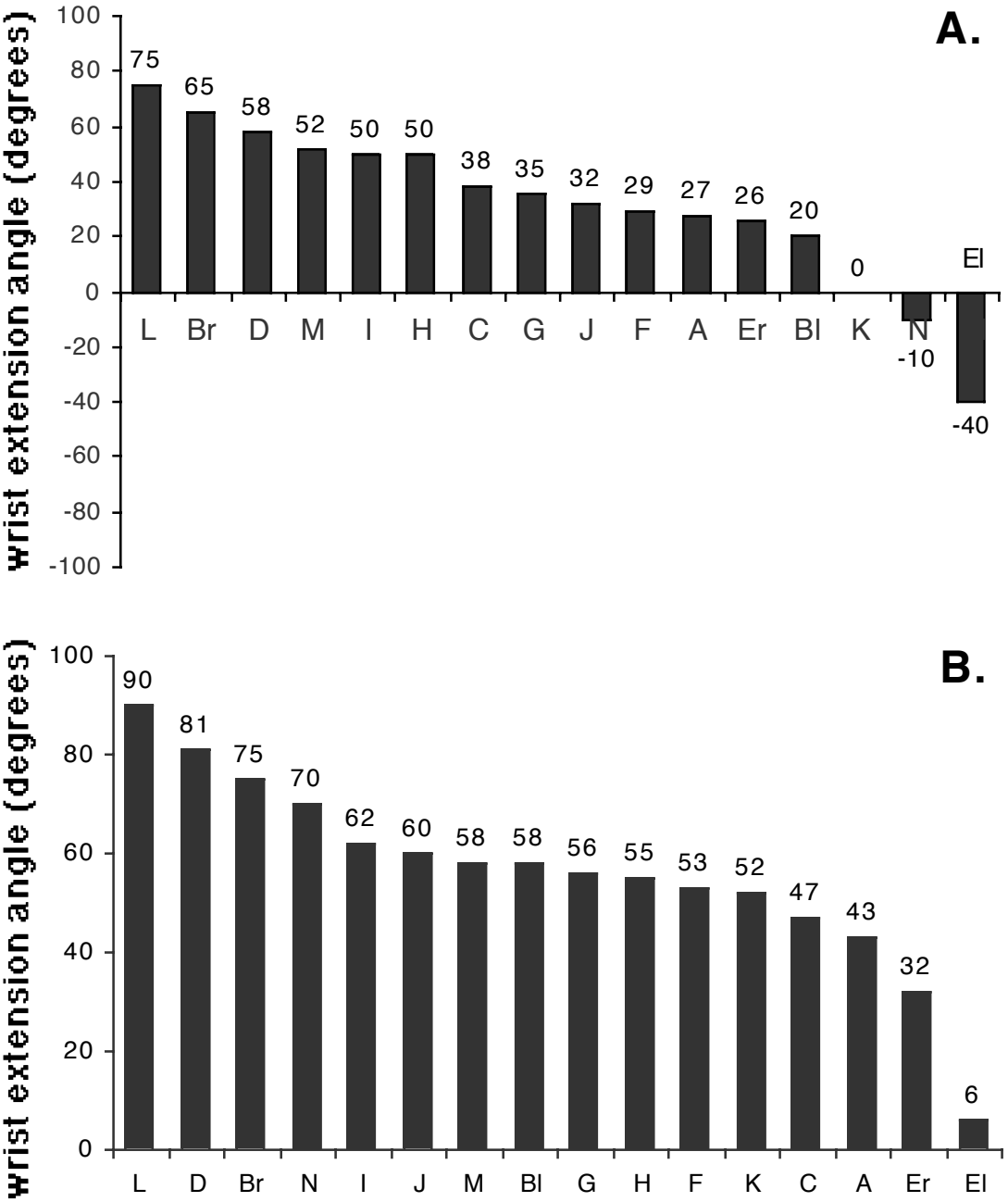

Fig. 1.b.1. (A). The maximum position in wrist extension that could be actively maintained against gravity in 16 wrists (from 14 individuals) with a Br-ECRB tendon transfer. Positive numbers indicate wrist extension, negative numbers indicate wrist flexion. The active range of motion in wrist extension varied substantially across wrists. Three individuals could not actively position their wrist in extension against gravity. (B). The passive limit of wrist extension in the same 16 wrists. Like the active range of motion, the passive range of motion varied substantially across wrists. All 16 wrists could be passively positioned in an extended wrist posture.

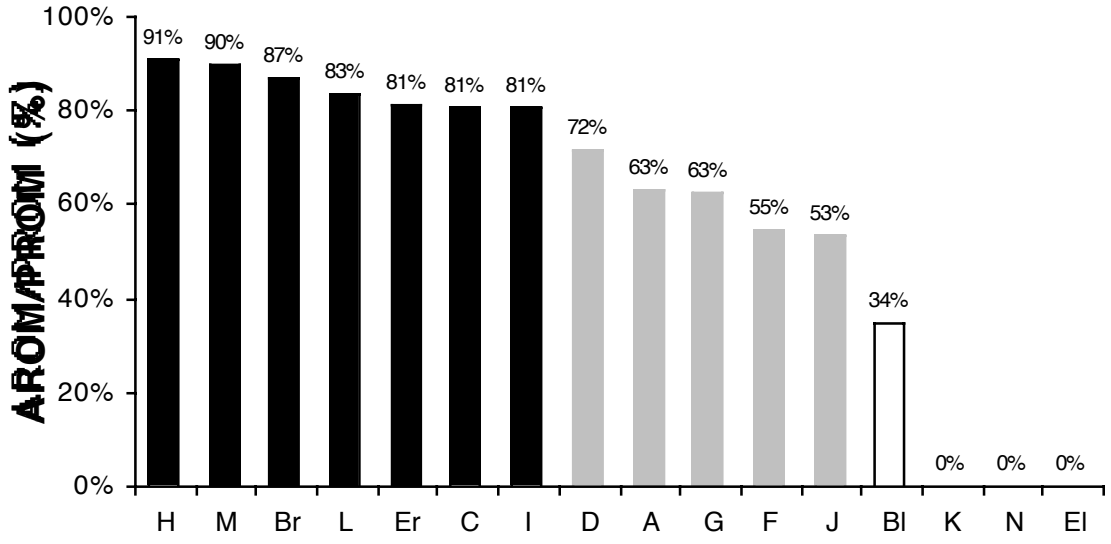

Fig. 1.b.2. The active range of motion (AROM) against gravity in wrist extension normalized by the passive range of motion (PROM) in wrist extension. The 16 wrists in this study were categorized into three groups based on this normalization. Group I (black bars, seven wrists) had an AROM that was greater 75% of the available PROM. Group II (gray bars, 5 wrists) had an AROM that was greater than 50% but less than 75% of the available PROM. Group III (white bars, 4 wrists) had an AROM that was less than 50% of the available PROM.

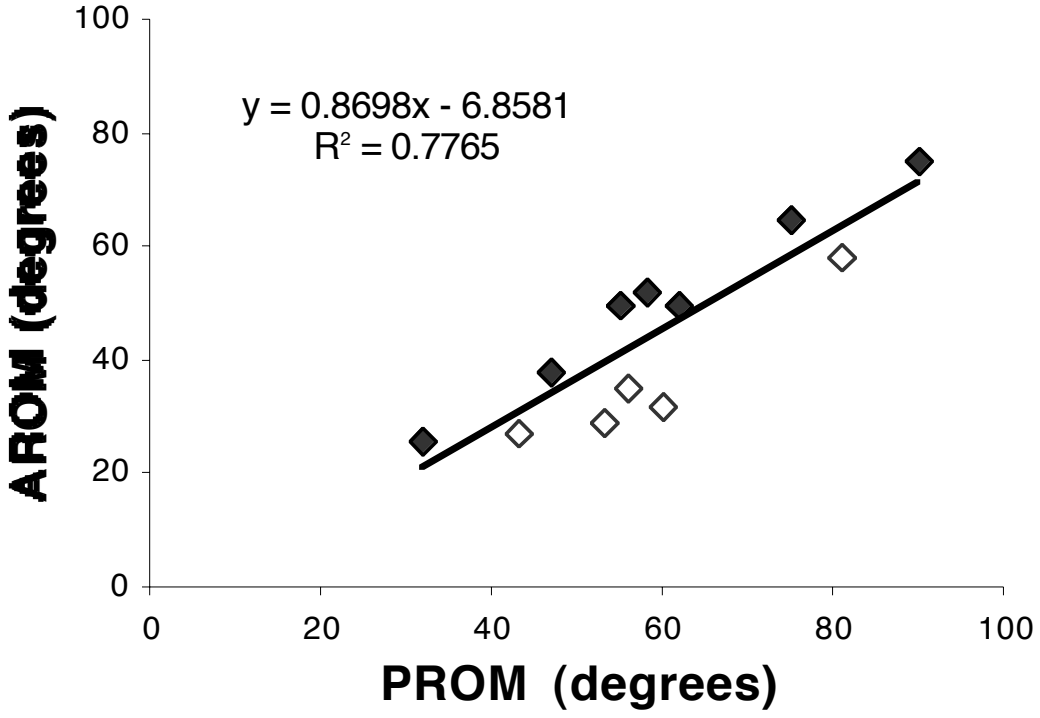

Fig. 1.b.3. The active range of motion (AROM) against gravity in wrist vs the passive range of motion (PROM) in wrist extension for the 12 wrists in Group I (filled diamonds) and Group II (open diamonds). The AROM in wrist extension was significantly correlated to the PROM in wrist extension in these 12 wrists.

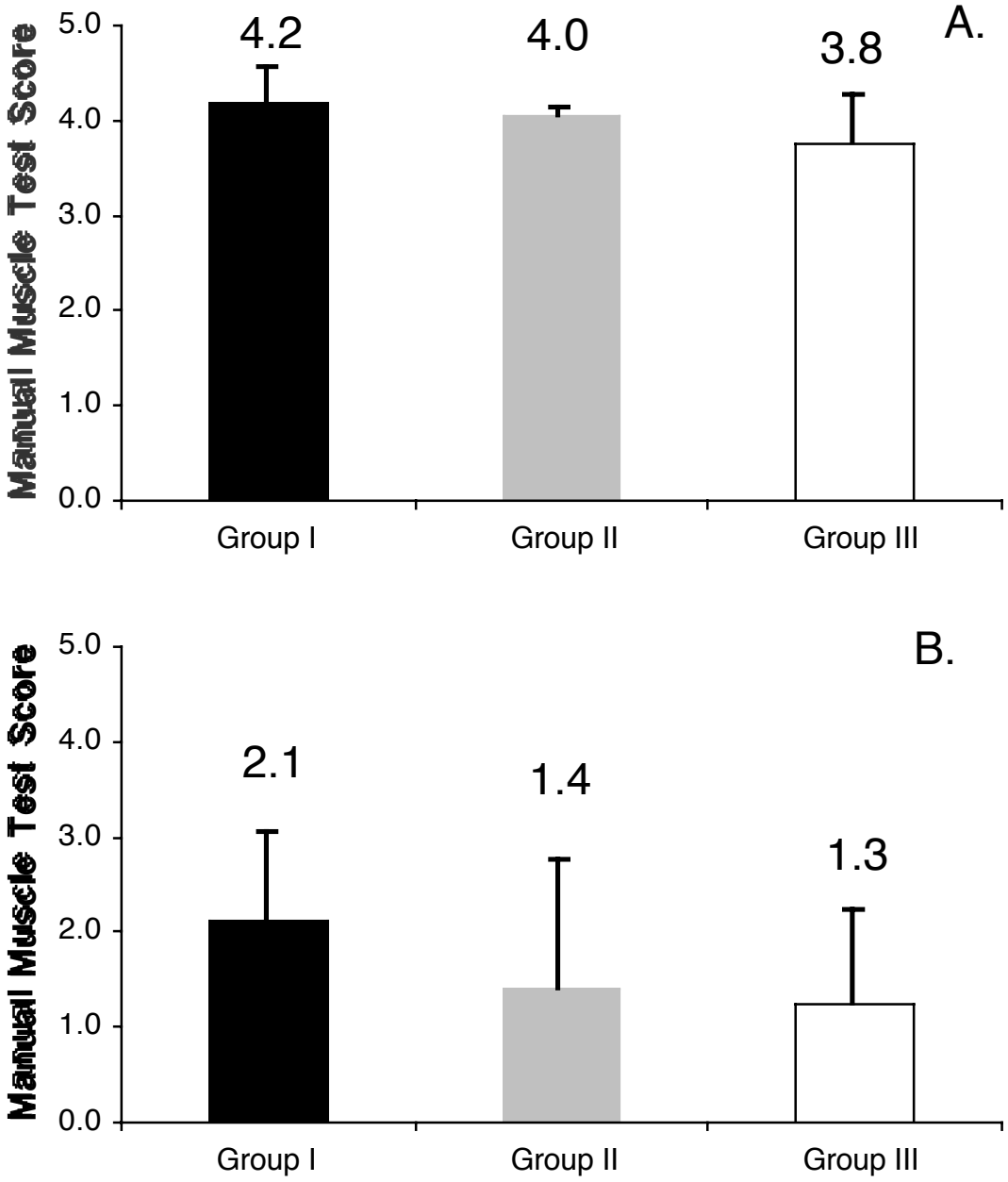

Fig. 1.b.4. (A). The average, pre-operative manual muscle test scores for the brachioradialis function at the elbow for the wrists in Group I (black bar, seven wrists), Group II (gray bar, five wrists), and Group III (white bar, 4 wrists). No significant differences in manual muscle test scores were found across the three groups. (B). The average, pre-operative manual muscle test scores for the wrist extensors for the wrists in Group I (black bar), Group II (gray bar), and Group III (white bar). No significant differences in manual muscle tests were found across the three groups. Error bars for A and B show one standard deviation.

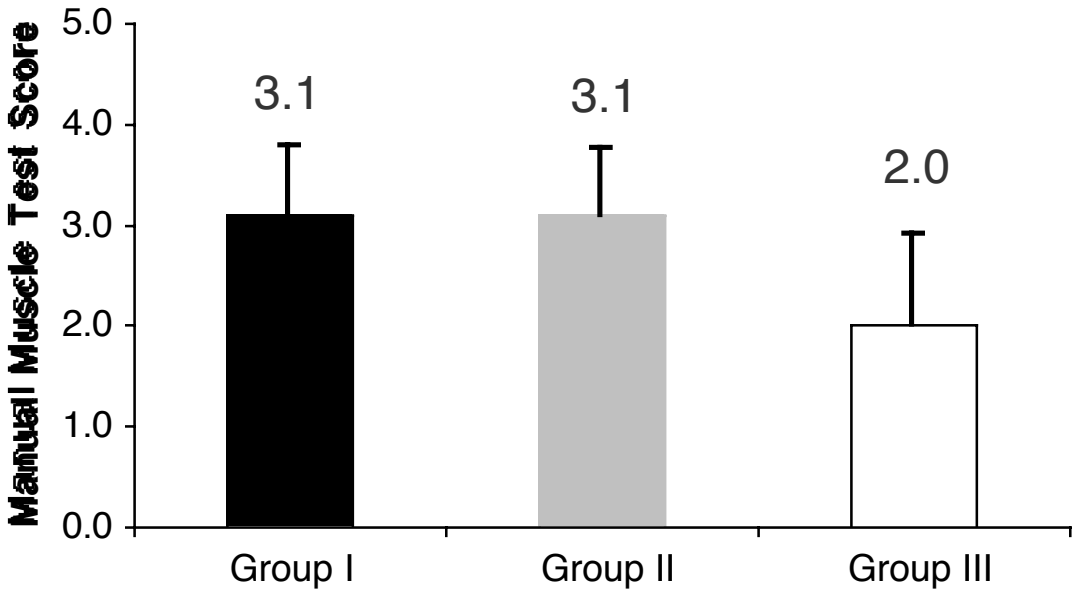

Fig. 1.b.5. (A). The average, post-operative manual muscle test scores for wrist extensors for the wrists in Group I (black bar, seven wrists), Group II (gray bar, five wrists), and Group III (white bar, 4 wrists). No significant differences in manual muscle test scores were found across the three groups. Error bars show one standard deviation.

Plans for Next Quarter

In the next quarter, we plan to begin quantitative measurements of wrist extension strength, elbow extension strength, and passive joint properties in individuals with Br-ECRB transfers.

2. CONTROL OF UPPER EXTREMITY FUNCTION

Our goal in the five projects in this section is to either assess the utility of or test the feasibility of enhancements to the control strategies and algorithms used presently in the CWRU hand neuroprosthesis. Specifically, we will: (1) determine whether a portable system providing sensory feedback and closed-loop control, albeit with awkward sensors, is viable and beneficial outside of the laboratory, (2) determine whether sensory feedback of grasp force or finger span benefits performance in the presence of natural visual cues, (of particular interest will be the ability of subjects to control their grasp output in the presence of trial-to-trial variations normally associated with grasping objects, and in the presence of longer-term variations such as fatigue), (3) demonstrate the viability and utility of improved command-control algorithms designed to take advantage of forthcoming availability of afferent, cortical or electromyographic signals, (4) demonstrate the feasibility of bimanual neuroprostheses, and (5) integrate the control of wrist position with hand grasp.

2. a. HOME EVALUATION OF CLOSED-LOOP CONTROL AND SENSORY FEEDBACK

Abstract

The purpose of this project is to deploy an existing portable hand grasp neuroprosthesis capable of providing closed-loop control and sensory feedback outside of the laboratory. We have completed the development of a stand alone, analog, single channel stimulator for grasp-force feedback. The field tests for of the prototype unit described in the prior report were delayed and will be pursued in the forthcoming quarter.

Purpose

The purpose of this project is to deploy a portable hand grasp neuroprosthesis capable of providing closed-loop control and sensory feedback outside of the laboratory. Our goal is to evaluate whether the additional functions provided by this system benefit hand grasp outside of the laboratory.

Progress Report

No progress to report this quarter.

Plans for Next Quarter

As originally planned for the previous quarter, we will make a set of short-run (1 day) field tests of the α-prototype on neuroprosthesis users in order to detect and correct remaining design problems. We are particularly concerned about the ergonomics of the sensor and electrode. Pending successful completion of the tests, we will produce 5-6 units for field deployment.

2. b. INNOVATIVE METHODS OF CONTROL AND SENSORY FEEDBACK

2. b. i. ASSESSMENT OF SENSORY FEEDBACK IN THE PRESENCE OF VISION

Abstract

No additional experimental work was completed this quarter. The manuscript describing the study completed in the previous quarter has now been accepted in *Medical and Biological Engineering and Computing*. The primary objective for the next quarter is to improve documentation and organization of the rather complex software in order to make the video-simulation system accessible to new users.

Purpose

The purpose of this project is to develop a method for including realistic visual information while presenting other feedback information simultaneously, and to assess the impact of feedback on grasp performance. Vision may supply enough sensory information to obviate the need for supplemental proprioceptive information via electrocutaneous stimulation. Therefore, it is essential to quantify the relative contributions of both sources of information.

In this quarter, we completed basic bench-top evaluations of the completed, prototype, single-channel, grasp-force feedback system. These evaluations were necessary prior to field testing to confirm that the output of the device was within the desired range, that the static transfer function approximated the desired mathematical relationship, and that the user adjustments modified the transfer function appropriately. The tests showed that the unit functioned roughly as specified, but that some specific fixed resistors will need different values to improve performance.

The measurements were made using the apparatus shown in Fig. 2.a.1. The force sensor (consisting of a force-sensing resistor mounted on a plastic thumb clip, with an overlying layer of foam and a thin aluminum contact plate, as described previously) was placed in series with a spring-loaded manipulandum (see Van Doren 1995) containing a commercial load cell (Entran ELF-1000), and compressed in a vise. Forces were measured with the commercial load cell, while the stimulator output was measured via a fixed load resistor (initially 1.022K) and an oscilloscope. Force-to-current transfer functions were measured for a variety of load resistors and control potentiometer settings.

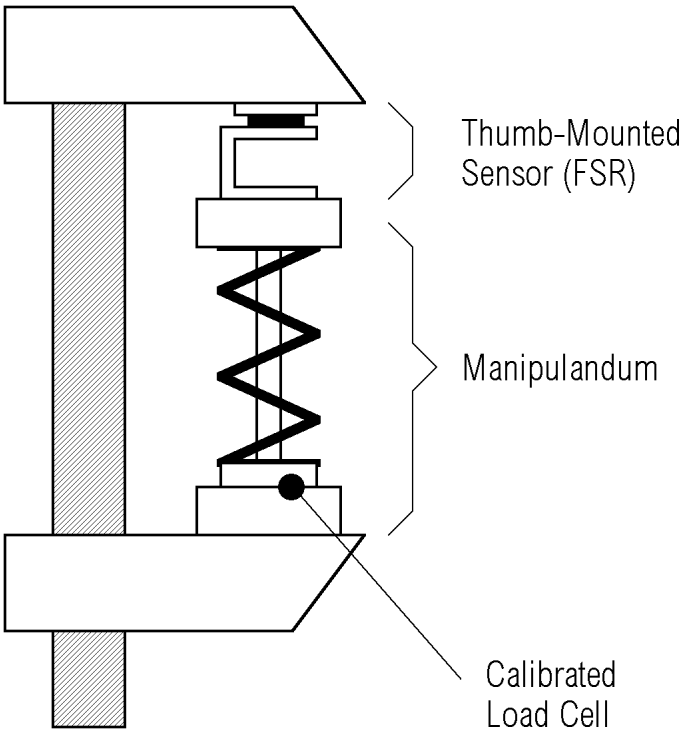

Fig. 2.a.1. Schematic drawing of apparatus used for testing force-feedback stimulator. The manipulandum assembly has been described previously.

The two control potentiometers change the exponent and scale factor of the transfer function (see Progress Report 9):

$$i = i_{\min}\left(F/F_{\min}\right)^{m} \qquad (2.a.1)$$

where $i_{\min}$ is a just-detectable stimulus current that is produced when the threshold force $F_{\min}$ is applied to the sensor. The potentiometers are adjusted by the user in the following sequence:

1. A fixed resistor corresponding to the value of the thumb sensor FSR under a load of $F_{\min}$ is connected to the stimulator input in lieu of the thumb sensor.
2. The user adjusts the “threshold” potentiometer to produce a just-detectable stimulus
3. The thumb sensor is connected and the user applies a maximum voluntary force (or, another fixed resistor may be used with an appropriate value)

4. The user adjusts the “exponent” potentiometer to produce the maximum comfortable stimulus amplitude.

This procedure relies on the independence of the threshold and exponent adjustments, and on the proper selection of fixed component values chosen for a particular thumb sensor. The purpose of the bench tests was to confirm circuit performance.

The first series of tests investigated the effects of changing the exponent given a fixed threshold. Static force-current transfer functions were acquired as described above for 4 settings of the exponent potentiometer (expressed as a fraction of the full range setting since the potentiometer was a linear slide potentiometer and actual resistances of the legs were not accessible for measurement) while the threshold adjustment was set at its minimum. The results are shown in Figure 2.a.2. The transfer functions all intersect at a point consistent with independence of the threshold and exponent, but the intersection is not at the force originally specified during circuit construction (i.e. 2N) and the transfer functions are not power functions (which would appear as straight lines in the figure). The latter discrepancy is no doubt due to errors in approximating the FSR response (i.e. resistance as a function of force) as a power function (see PR9). The discrepancy is not severe, however, and the transfer function is satisfactory. It may be useful to reduce the range of exponent variation (e.g. configure potentiometer to yield 25-100% range) to achieve more sensitive control. The threshold error, however, is significant (roughly 3 versus 2 N — an error of 50%) and will require revising the internal threshold calibration resistor.

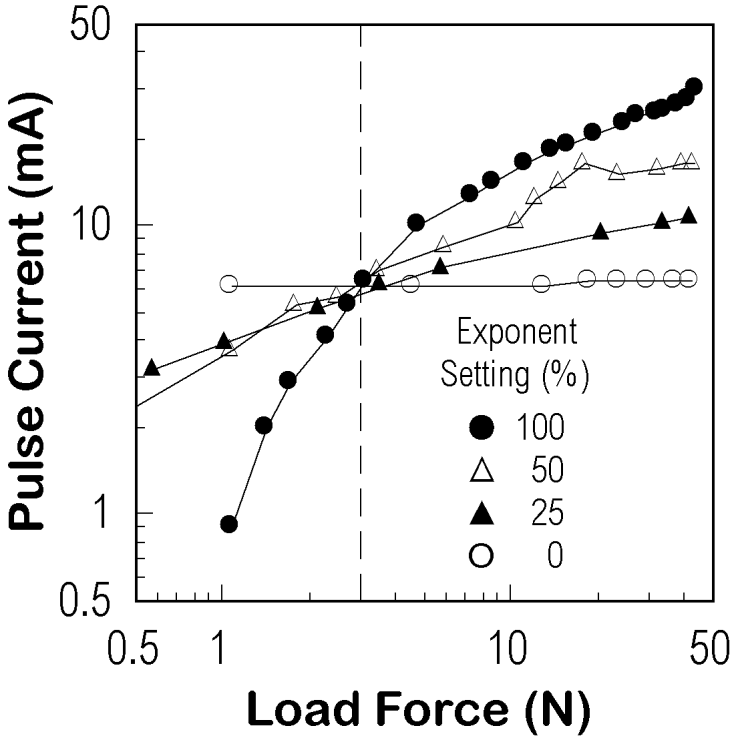

Fig. 2.a.2 Plots of stimulus pulse current into a 1K load as a function of load force for different settings of the transfer function exponent. The threshold setting was fixed at its minimum. Note that, as anticipated, the functions intersect at (what is defined as) the “threshold” force (dashed line).

Analogous results for variations in the threshold parameter are shown in Fig. 2.a.3. The data for the minimum setting have been replotted from Fig. 2.a.2. Mathematically, a change in the threshold (i_{min}) should only shift the functions vertically, without a change in shape. That behavior is approximately true, although there is a pronounced saturation at the maximum stimulus current. Note, however, that the range of adjustment is extremely narrow. The useful range is from roughly 0-8% of the full range. Threshold values between 10% and 100% produce nearly the same transfer function. This result is important since the threshold adjustment is especially sensitive subjectively. As a consequence, the configuration and value of the threshold potentiometer will have to be revised before entering into field trials with naive users.

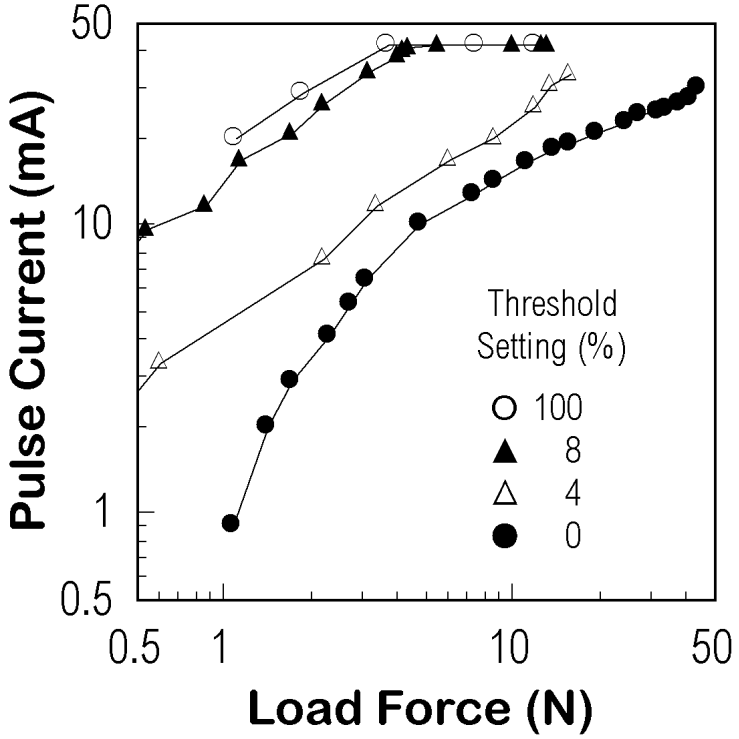

Fig. 2.a.3. Plots of output current versus load force, as in Fig. 2.a.2., but for variations in the setting of the threshold current parameter. Note that most of the output variation occurs over a very narrow range of parameter settings (0-8%).

As an additional test of circuit behavior, we tested simultaneous changes in both exponent and threshold parameters. Our goal was to increase the stimulus amplitudes at low forces without affecting amplitudes at high force. Based on the preceding measurements, we chose values of 4% of threshold range and 25% of exponent range, producing the transfer function shown in Fig. 2.a.4. Note that the adjustment, in effect, lowered the *force* threshold (i.e. the force at which the minimum detectable current is produced) without affecting the maximum output, as desired.

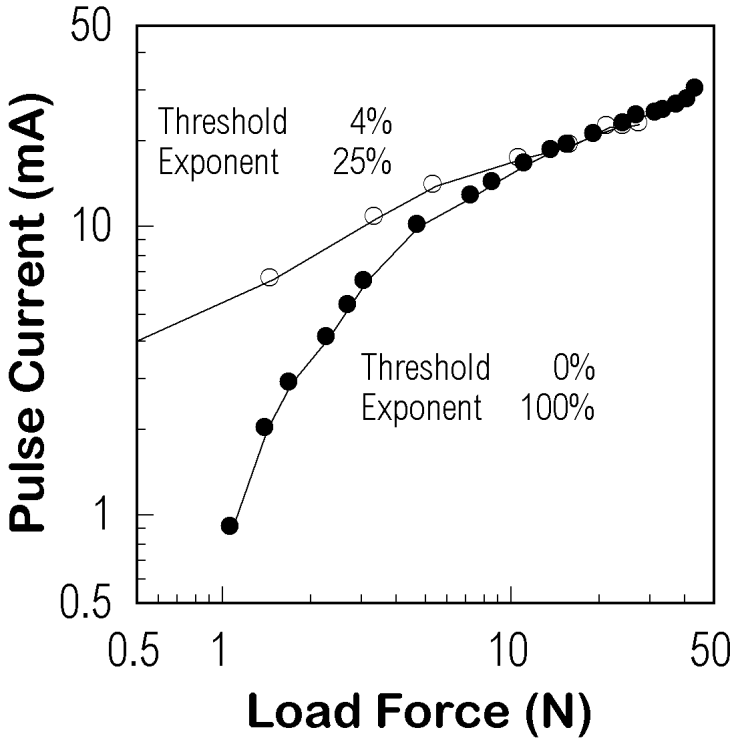

Fig. 2.a.4 Plot of output current as function of load force for simultaneous change of both threshold and exponent settings.

The final test in this suite was to measure the output current as a function of load resistance to verify the constant-current behavior. The results are shown in Fig. 2.a.5 for load resistances ranging from 1 to 50K. Note that the output current is indeed constant (in this case, 10 mA) for loads up to 10K, and then drops as the output reaches its maximum voltage (122V).

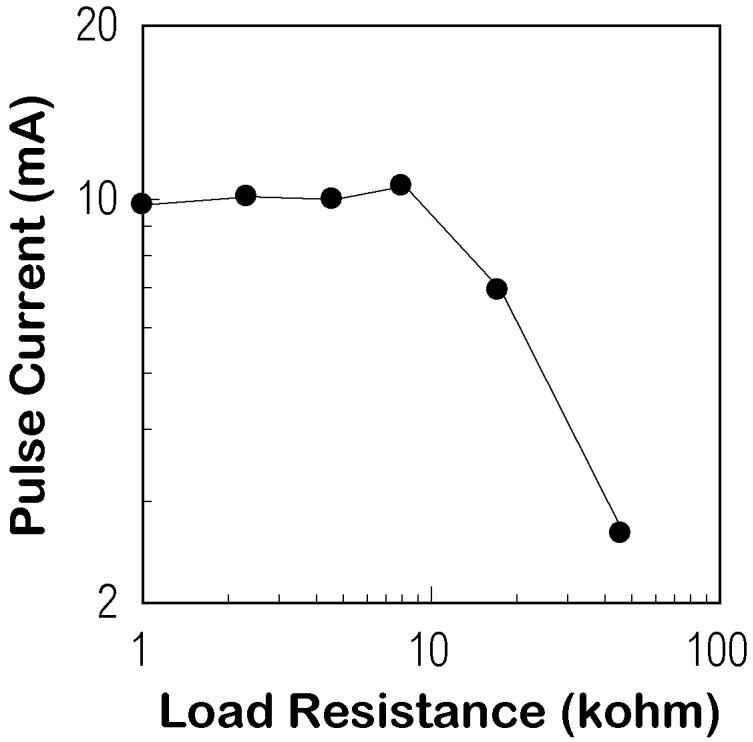

Fig. 2.a.5. Output current as a function of load resistance.

Plans for Next Quarter

The values and configurations of the exponent and threshold adjustment potentiometers will be revised and tested. Additional thumb sensors will be fabricated, requiring improved flexibility in setting the calibration resistor internal to the stimulation unit. Also, we anticipate contacting a hand neuroprosthesis user in Oklahoma who has been selected as most appropriate for small-scale field trials.

Reference:

Van Doren CL (1995) Pinch force matching errors predicted by an equilibrium-point model *Exp Br Res* 106:488-492

2. b. ii. INNOVATIVE METHODS OF COMMAND CONTROL

Abstract

The purpose of this project is to develop new command control algorithms that will make control of neural prosthetic hand grasp simpler and more effective. During this quarter testing was conducted on seven command control algorithms across five subjects. The results from these tests are being compared using multifactor ANOVAs and using generalized estimating equations.

Purpose

The purpose of this project is to improve the function of the upper extremity hand grasp neuroprosthesis by improving user command control. We are specifically interested in designing algorithms that can take advantage of promising developments in (and forthcoming availability of) alternative command signal sources such as EMG, and afferent and cortical recordings. The specific

objectives are to identify and evaluate alternative sources of logical command control signals, to develop new hand grasp command control algorithms, to evaluate the performance of new command control sources and algorithms with a computer-based video simulator, and to evaluate neuroprosthesis user performance with the most promising hand grasp controllers and command control sources.

Progress Report

1. Command Control Algorithms

Explanations of and state diagrams describing the baseline, lock only (LO), proportional rectified-lock (PRL), threshold rectified-lock (TRL), and variable-gain (VG) algorithms were given in previous progress reports.

The variable-gain rectified-lock (VGRL) algorithm is similar to the variable gain algorithm. Figure C.2.b.ii.1 shows the state diagram for this algorithm. Like the variable-gain algorithm, when the subject locks the hand and returns to the zero position of the control shoulder, the remaining hand range is remapped over the entire control shoulder range. When the subject then elevates the control shoulder over the zero position, the hand closes proportionally and the locked value of the hand is re- set at the new higher value. If the subject chooses to return the control shoulder to the zero position again, then the hand is re-zeroed at the new locked value and the remaining hand range is remapped over the entire control shoulder range.

The threshold gated ramp (TGR) algorithm, operates using two control shoulder position thresholds. While the subject's shoulder position exceeds the first threshold and is below the second, the command signal is linearly ramped down, thus opening the hand or decreasing the grip force until the shoulder leaves this range or the hand reaches its zero position. While the control shoulder exceeds the second threshold, the command level is ramped upward, thus increasing the force or decreasing the opening of the hand. A state diagram for this algorithm is also shown in figure C.2.b.ii.1.

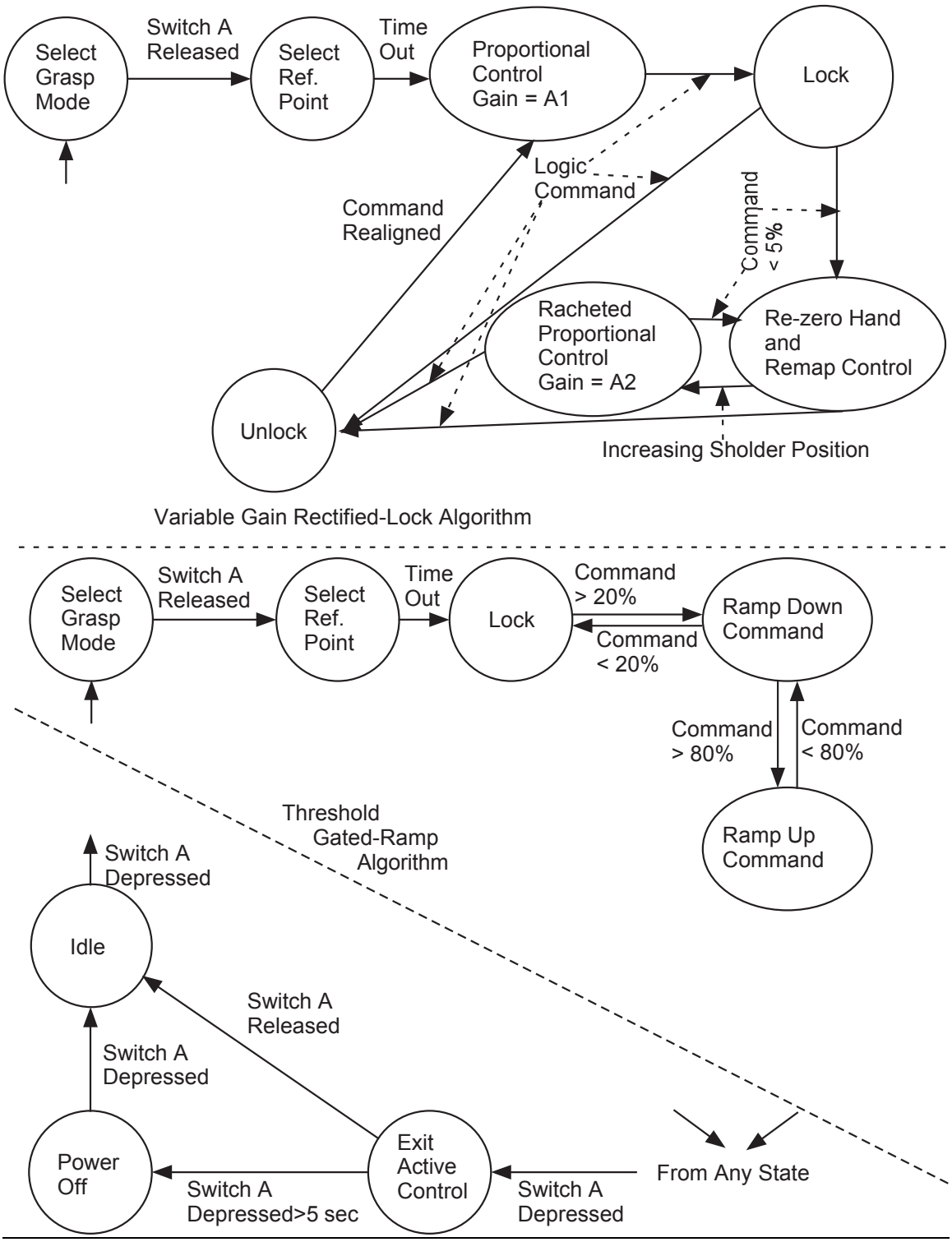

Figure C.2.b.ii.1 State diagram for the variable-gain rectified-lock and threshold gated-ramp algorithms.

2. Command Control Algorithm Testing

Testing of seven command control algorithms was conducted on five subjects, three male and two female, between the ages of 22 and 29. Each subject participated in at least seven sessions. These sessions were divided into two sets of three sessions and at least one practice session. Each subject tested every algorithm once in each set of sessions. Before the first set of trials, any subjects that were not familiar with the video simulator were required to participate in a one hour practice session to familiarize the user with controlling the system. Since there was about a month between the end of the first set of sessions and the beginning of the second set, every subject was required to participate in a 1.5-2 hour practice session. Each set of sessions was conducted within a one week period for each subject, except for two subjects who needed longer in the first set. Table C.2.b.ii.1 presents the order in which the algorithms were tested for each subject. For brevity, the algorithms are numbered: 0-baseline, 1-LO, 2-PRL, 3-TRL, 4-VG, 5-VGRL, 6-TGR.

Table C.2.b.ii.1 Order of presentation of the command control algorithms during testing sorted by subject, session, and order within session.

Subject #	Session 1	Session 2	Session 3	Session 4	Session 5	Session 6	Session 7
1	0,5,1	0,3,4	0,2,6	0,0,0	0,6,3	0,1,2	0,4,5
2	0,6,3	0,1,2	0,4,5	0,0,0	0,2,5	0,4,6	0,1,3
3	0,2,5	0,4,6	0,1,3	0,0,0	0,1,4	0,5,6	0,3,2
4	0,1,4	0,5,6	0,3,2	0,0,0	0,2,4	0,3,5	0,6,1
5	0,2,4	0,3,5	0,6,1	0,0,0	0,5,1	0,3,4	0,2,6

3. Testing Results

Each subject completed the acquire-hold-modify task described previously using each of the command control algorithms. Success rate curves for each algorithm, pooled across data sets are shown in figure C.2.b.ii.2. Curves A through E show the results for each subject, and curve F shows the results pooled across subjects. Clearly, the success rates were dependent on the subject, force window size, and the algorithm, but it was not clear from these curves which algorithms were the best or worst. Therefore, our current efforts are directed at statistical analysis of the data.

Two different methods are being used to analyze this data. The first is to apply an arcsine transform to the data, which provides a uniform power distribution for the effect size over the range of the data. Doing so allows the data to be analyzed using a repeated measures ANOVA model.

The second analysis being performed is a linear model using generalized estimating equations (GEEs) to find the coefficients. Since the data is both binary and uses repeated measures, the use of an ANOVA or any linear model without GEEs could not be used. Therefore, a linear model with GEEs is being used to model the data.

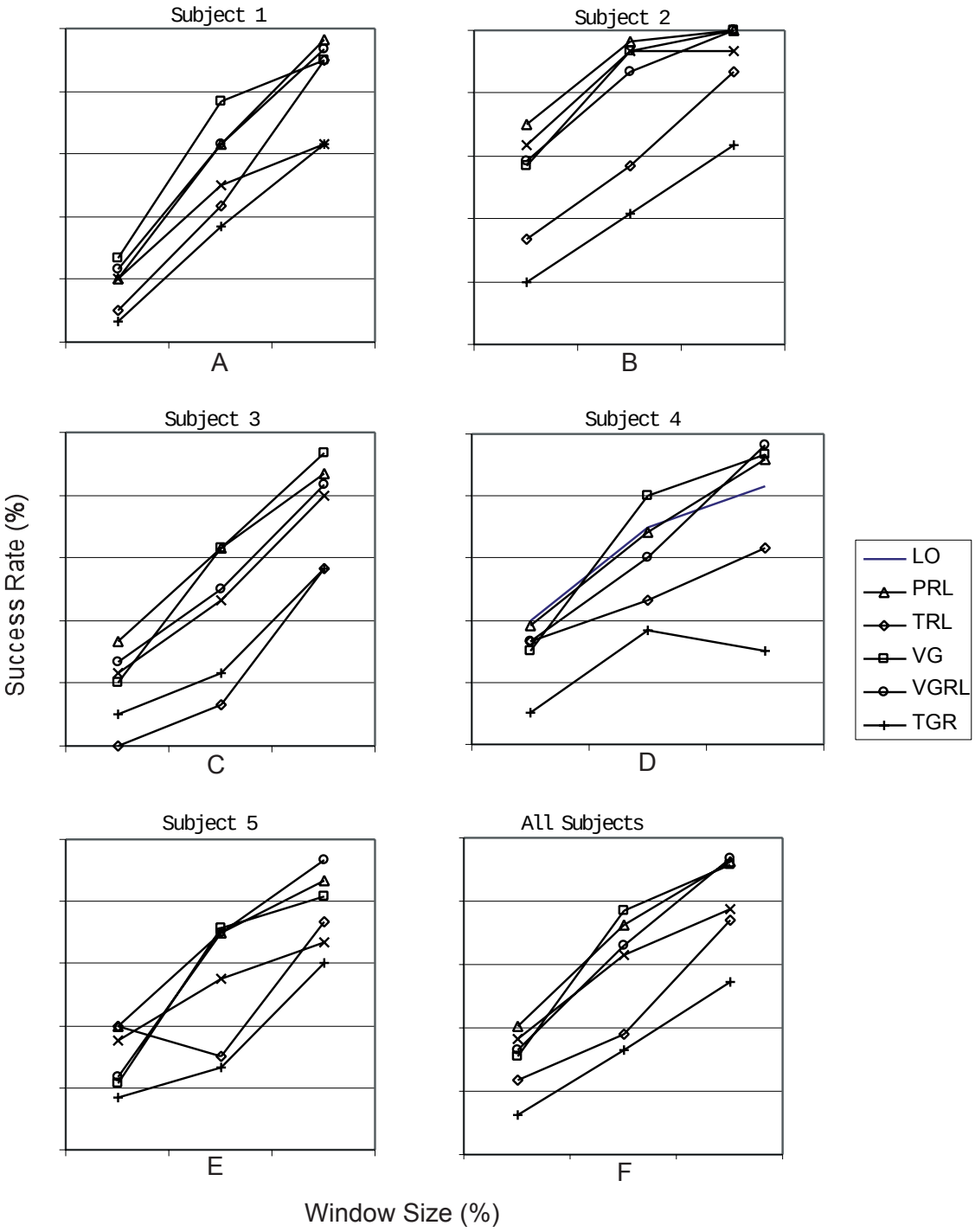

Figure C.2.b.ii.2 Success rate curves for the six command control algorithms being compared. Each curve is pooled across data sets for each session. Curves A-E are for each of the subjects in the study. Curve F is pooled across all subjects.

Plans for Next Quarter

In the next quarter, the statistical analysis using the ANOVAs and generalized estimating equations will be completed. Program documentation will also be completed.

2. b. iii . INCREASING WORKSPACE AND REPERTOIRE WITH BIMANUAL HAND GRASP

Abstract

Development of an EEG interface for the hand grasp neuroprosthesis was completed. The interface allows development of several algorithms to convert the EEG signal into a command to operate the neuroprosthesis. Currently, two algorithms have been designed, based upon the binary nature of the EEG signal. One of the algorithms, the hold switch method, has been tested with one neuroprosthesis user with a Grasp and Release Test (GRT). Results indicate that the rate of performance in the GRT is modest and relatively consistent across objects, and that there are certain inherent delays that limit the rate at which a user can operate the system.

Purpose

The objective of this study is to extend the functional capabilities of the person who has sustained spinal cord injury and has tetraplegia at the C5 and C6 level by providing the ability to grasp and release with both hands. As an important functional complement, we will also provide improved finger extension in one or both hands by implantation and stimulation of the intrinsic finger muscles. Bimanual grasp is expected to provide these individuals with the ability to perform over a greater working volume, to perform more tasks more efficiently than they can with a single neuroprosthesis, and to perform tasks they cannot do at all unimanually.

Progress Report

During the last quarter, the efforts on this project were shifted from the training of the frontal beta rhythm and analysis of the signal to the further development of an EEG-based interface to the hand grasp neuroprosthesis. In a previous report (January 1999), a rudimentary interface between the BCI system developed by Wolpaw and the hand grasp system was described. However, this interface had several limiting factors. The most important of these was that the interface prevented direct access to the EEG voltages and thus limited the development of algorithms to convert the EEG signal into an appropriate command for the neuroprosthesis. To circumvent these problems, it was necessary to bypass the BCI system and condense the entire signal processing on a single computer. In this manner, it would then be possible to access the data needed for adequate algorithm development.

The interface that was developed in represented schematically in Figure 2.b.iii.1. As can be seen from the figure, only one computer was involved in collecting the data from the EEG amplifier, processing the signal, and interfacing with the hand grasp neuroprosthesis. This was accomplished with the LabVIEW programming language and a PC-LPM-16/PnP data acquisition (DAQ) board from National Instruments. The DAQ has allowed for the sampling of 16 channels of data (although only 5 are required) at a sufficient rate to allow for neuroprosthetic operation. Through control by the LabVIEW program, the EEG signals were sampled at a 1 kHz sampling rate, the Laplacian spatial filter was applied, and the power spectra of the EEG was calculated using a Fast Fourier Transform. It was then possible to derive the EEG voltage from the beta band (24 – 29 Hz), which was then used as the input into a control algorithm.

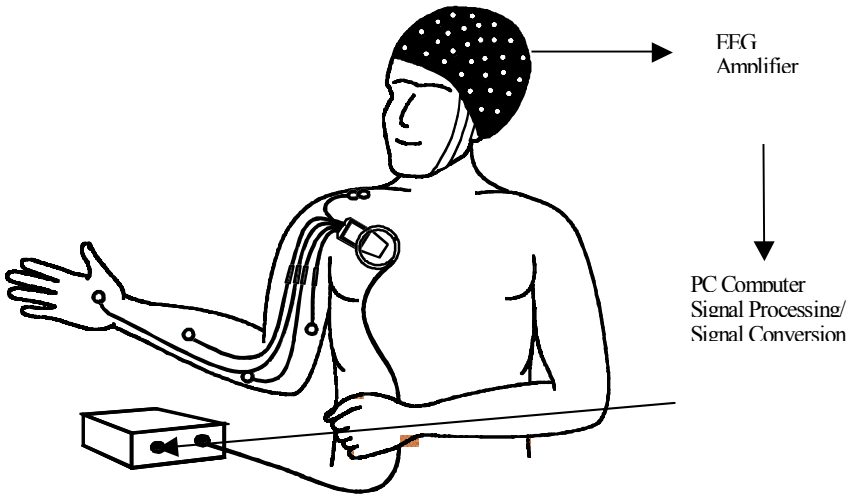

Figure 2.b.iii.2 – Schematic of the EEG interface to neuroprosthesis

The LabVIEW program was also used to convert the EEG signal into a command for the neuroprosthesis. The first step in this process was the application of an additional low pass filter. For this, the adaptive step size filter was used to function as an n-point smoother on the EEG signal to eliminate some of the intermittent voltage spikes that were generated and were not under the control of the user. The filtered signal was then used the input to the control algorithm for conversion to a command-control signal. Currently, there are two algorithms that have been developed. The first was the hold switch algorithm, and the second was the toggle algorithm. Both of these were based upon a binary input signal since it has only been possible to distinguish two distinct levels of control in the EEG with any degree of reliability, a resting baseline level and a low voltage (suppression of EEG activity) level.

The operation of the hold switch algorithm is represented in Figure 2.b.iii.2. The name of the algorithm refers to its mode of operation. In this case, the hand closes and remains closed for as long as the "switch" is closed (i.e. the low EEG voltage is maintained). As soon as the switch is released, the hand responds by opening once again. This algorithm can also be inverted so that the hand starts in a closed position, and opens for as long as the switch is held. Also represented by the figure is the 250 ms delay between the time the EEG signal changes and when the command begins to change. This delay was necessary since with the EEG signal there can occur periods of time which last between 100 and 200 ms where there is no beta activity. This is naturally occurring phenomenon, and not under the

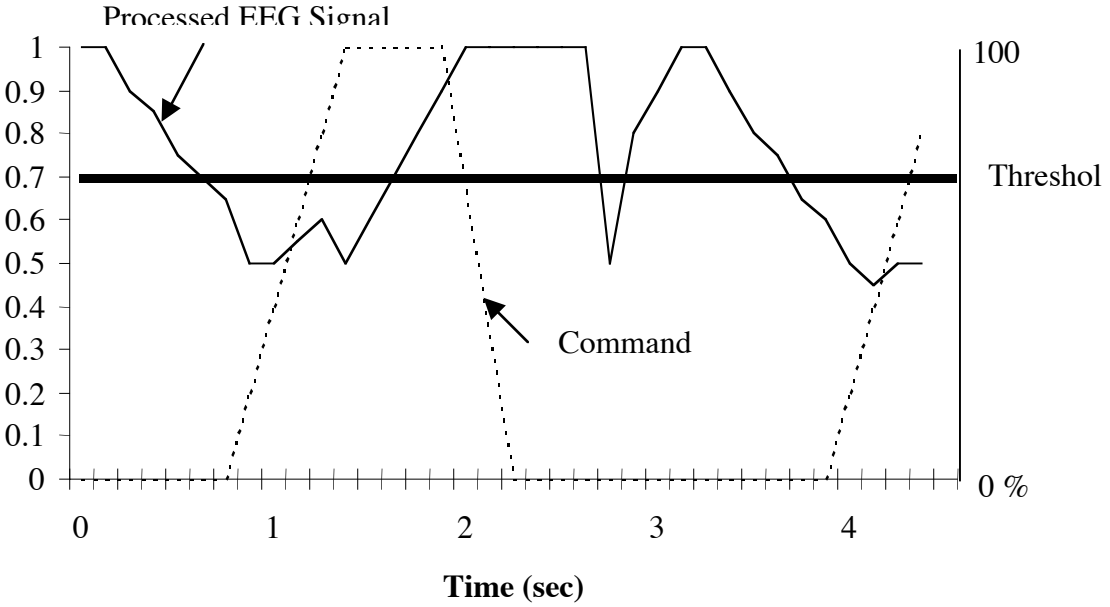

Figure 2.b.iii.4 - Example of Hold Switch Algorith

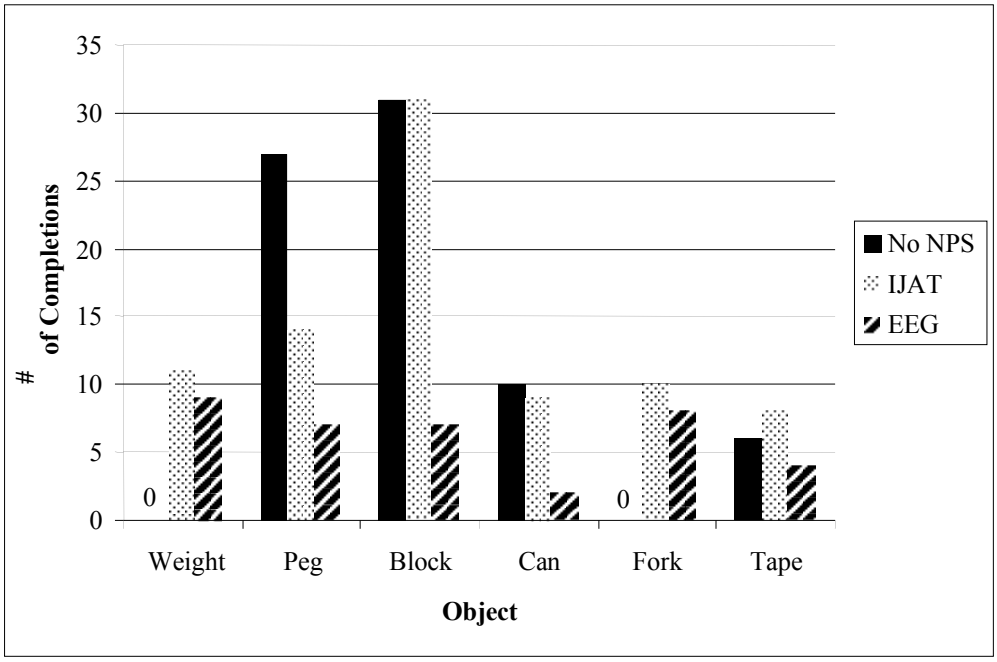

Figure 2.b.iii.3 - Comparison on GRT with EEG interface, IJAT and no neuroprosthesis

conscious control of the user. If the delay were not present, then these periods of no activity would generate an unwanted command to close the hand.

The second algorithm that has been developed is the toggle algorithm. This algorithm, as stated earlier, is also based upon the binary nature of the EEG. However, it differs for the hold switch algorithm in that it allows for the neuroprosthesis user to lock the hand in position without having to maintain a given level of EEG activity. Similar to the hold switch algorithm, the hand starts in the open position. When the EEG level is suppressed and exceeds the low threshold level, the hand closes at a fixed rate. Once full hand closure is achieved, the user can relax and the hand will remain in the closed position. If the user desires to open the hand, the subject suppresses the beta rhythm activity below the threshold, which will generate the command to open the hand.

The capabilities of the EEG interface have been tested using a performance test for hand function. To date, only the hold switch algorithm has been evaluated with one neuroprosthesis user. The subject initially spent three to four sessions learning to use the EEG signal to operate his neuroprosthesis. Once the subject felt comfortable in its use, the Grasp and Release Test was used to assess how well the EEG controller compared to the subjects "standard" controller. The GRT is a test that has been developed by our laboratory to access the capabilities of different control methods for the neuroprosthesis. In this test, the object is to manipulate six objects of varying sizes and weights as many times as possible during a fixed time interval. For evaluation purposes, the "standard" controller that the EEG interface was compared to was the implanted joint angle transducer (IJAT) in the wrist. The results of this comparison on the GRT are shown in Figure 2.b.iii.3. Also represented in the figure are the results of this subject on the GRT when he is not using the neuroprosthesis. The result shows several aspects of the neuroprosthesis performance and some limitations of the EEG controller. First, performance on the light objects (the peg and block) was much better without the neuroprosthesis than with the system. However, this result is somewhat misleading in that with the light objects, the neuroprosthesis is not used. In is only in the manipulation of heavier objects, or when it is desired to maintain a grasp upon an object, that an individual uses the system. This advantage of the neuroprosthesis is clearly seen with the heavier objects of the GRT (such as the weight and the fork). The second observation to be made is that performance of the EEG controller for the heavier objects approaches the performance of the IJAT. This result was unexpected, but encouraging, since it was believed that the EEG controller would be much slower than the IJAT on a timed manipulation test like the GRT. However, it can be seen that there is a limitation in performance of the EEG controller, based on the fact that approximately the same number of objects are manipulated in the 30 second trial of the GRT regardless of hand grasp used and the weight of the object. Where the delays in the controller occur at this point are unknown, but are expected to lie mostly in the generation of the EEG voltage by the individual to drive the neuroprosthesis.

Plans for Next Quarter

During the next quarter, experiments will be conducted to determine the source of the delays in the EEG controller and their length. The neuroprosthesis user will also be trained using the other algorithm, and the performance of this control strategy will also be assessed using the GRT.

2. b. iv CONTROL OF HAND AND WRIST

Abstract

We are specifying and developing hardware and software to implement both a laboratory and a portable neuroprosthesis for feedforward neural network control of hand grasp and wrist angle. We are currently evaluating the suitability of operating systems and commercial software packages to reduce the design/implementation time required to implement novel systems.

Purpose

The goal of this project is to design control systems to restore independent voluntary control of wrist position and grasp force in C5 and weak C6 tetraplegic individuals. The proposed method of wrist command control is a model of how control might be achieved at other joints in the upper extremity as well. A weak but voluntarily controlled muscle (a wrist extensor in this case) will provide a command signal to control a stimulated paralyzed synergist, thus effectively amplifying the joint torque generated by the voluntarily controlled muscle. We will design control systems to compensate for interactions between wrist and hand control. These are important control issues for restoring proximal function, where there are interactions between stimulated and voluntarily controlled muscles, and multiple joints must be controlled with multijoint muscles.

Progress Report

In this quarter, after we looked at the performance and compatibility characteristics of three operating systems: Windows 95, Windows NT and Linux. Windows NT was selected as the platform for this system.

- Windows NT provides the capability to change the priority in which the system's tasks are executed.
- Windows NT offers real time performance in the range of milliseconds, having an average timer cycle of 35us, and the slowest timer cycle of 670us.
- Windows 95 does not offer the capability to prioritize tasks, nor is it a robust system (if an application crashes, the whole system crashes).
- Windows NT is an off-the-shelf operating system, which results in a great reduction in development costs and training time, as well as future compatibility.
- Linux requires a Real-time separated kernel to provide real-time performance; this goes against the off-the-shelf principle.

After the operating system was selected, the feasibility of the system was determined by implementing a real-time test using a hardware-timed control algorithm written using Matlab Neural Networks Toolbox© to create and simulate the neural network, and LabView© to develop the rest of the control software. This control program uses the PCI-MIO National Instruments© data acquisition board installed on the PC.

The description of this test for one cycle is as follows:

1. The system must wait for a digital triggering signal to start the process. A timer in the data acquisition board that provides stable timing with minimum jitter produces this digital signal.
2. This digital signal triggers a data acquisition process in which analog data samples are collected from several input channels. The sampled data corresponds to the grasp command, grasp mode, wrist angle, and arm orientation.
3. The acquired analog data is used as an input to an artificial neural network. This data will be used as the command signal, which is fed to the artificial neural network to determine the next system action. The neural network returns the stimulation pulse-widths necessary to produce the selected action according to the inputs from the user.
4. The stimulation pulse-widths returned by the neural network are then sent to the RF board using the computer's serial port. The RF board then sends these pulse-widths to the implanted stimulator via a radio frequency link.

5. After the pulse-widths have been sent serially to the RF board, the system waits until the appearance of the next digital trigger (Step 1).

To accurately measure the time spent in each of the previous steps, several digital input-output lines on the MIO-board were used as markers or flags, setting a particular line to high (logic 1) whenever the particular software action we wanted to measure started, and then setting it back to low (0 logic) when this action ended. The total cycle time was the sum of all individual times for all steps in the cycle.

The results obtained are:

Step	**Additional Information**	**Min time measured (ms)**	**Max time measured (ms)**
Data acquisition	3 Analog channels	2.51	3.85
Data Analysis (ANN)	Single ANN, 3 layers, 20h.n.	9.10	10.78
Serial transmission	10 stimulation channels	15.74	16.50
Other delays	Digital I/O line change	0.1224	0.1874
Total time		***27.47***	***31.32***
Jitter		*+-0.1732*	*+-0.2860*

This means that if we want to keep the same characteristics used here, we can use a stimulation frequency up to 30Hz, which is well beyond of the current requirements.

After developing this test, which corresponds also to the normal operation phase of the system, and having proved the feasibility of the system, we focussed on software that would be used to train the ANN. The training phase was also implemented using Matlab Neural Networks Toolbox to create and train the neural network, and LabView to develop the rest of the software. This training program also uses the PCI-MIO National Instruments data acquisition board installed on the PC to control the internal timing and to collect the required training data.

The training phase consists of performing many different trials, in which the muscles are stimulated at different levels. First, the stimulation parameters are specified for the different grasp modes at different stimulation levels. This data is stored in a file for their use in each trial.

1. For each trial, the corresponding stimulation parameters are read from the previously stored file, and then they are sent to the stimulator via the computer's serial port. At the same time, wrist angle, forearm orientation, grasp force and grasp opening are recorded using the National Instruments board and then stored in a file for their later analysis.
2. After all the data has been collected for all trials, it is analyzed using LabView to calculate the training data set for the neural network. This data set corresponds to the stimulation pulse-widths used to stimulate the muscles and the responses (wrist angle, grasp force, grasp opening and arm orientation) produced by them.
3. Using the training data set, the neural network is then trained using Matlab's Neural Networks Toolbox to obtain the desired output responses according to the input from the user. Here, the

neural network must be able to respond correctly to input patterns used during the training, as well as to other inputs not used for the training.

Plans for next quarter

At this moment, we are ready to start testing the communication links between the system and the RF board using the external control unit (LECU). Exhaustive testing of this communication between the system and the LECU needs to be performed.